

## ECOLOGY

# Direct quantification of energy intake in an apex marine predator suggests physiology is a key driver of migrations

Rebecca E. Whitlock,<sup>1,2\*</sup> Elliott L. Hazen,<sup>3</sup> Andreas Walli,<sup>1</sup> Charles Farwell,<sup>4</sup> Steven J. Bograd,<sup>3</sup> David G. Foley,<sup>3†</sup> Michael Castleton,<sup>1</sup> Barbara A. Block<sup>1</sup>

2015 © The Authors, some rights reserved; exclusive licensee American Association for the Advancement of Science. Distributed under a Creative Commons Attribution NonCommercial License 4.0 (CC BY-NC). 10.1126/sciadv.1400270

Pacific bluefin tuna (*Thunnus orientalis*) are highly migratory apex marine predators that inhabit a broad thermal niche. The energy needed for migration must be garnered by foraging, but measuring energy intake in the marine environment is challenging. We quantified the energy intake of Pacific bluefin tuna in the California Current using a laboratory-validated model, the first such measurement in a wild marine predator. Mean daily energy intake was highest off the coast of Baja California, Mexico in summer (mean  $\pm$  SD, 1034  $\pm$  669 kcal), followed by autumn when Pacific bluefin achieve their northernmost range in waters off northern California (944  $\pm$  579 kcal). Movements were not always consistent with maximizing energy intake: the Pacific bluefin move out of energy rich waters both in late summer and winter, coincident with rising and falling water temperatures, respectively. We hypothesize that temperature-related physiological constraints drive migration and that Pacific bluefin tuna optimize energy intake within a range of optimal aerobic performance.

## INTRODUCTION

An understanding of ecosystem responses to a changing ocean environment is key to effective management of marine communities. Apex marine predators are of particular concern owing to their potential to induce marked shifts in the dynamics and function of marine communities via cascading effects on lower trophic levels (1, 2). For highly migratory species, identification of the mechanisms that underlie migration is an important step in predicting ecosystem-level responses to a warming ocean (3).

The study of physiological mechanisms that govern change in species' performance (foraging, growth, reproduction, etc.) can help to elucidate responses to climatic warming (4). In many animals, aerobic scope (the difference minimal and maximal rates of oxygen consumption) decreases with cooling or warming outside the optimum temperature range, resulting in lower performance (4, 5). Pacific bluefin tuna (*Thunnus orientalis*) is a highly migratory marine predator of acute conservation concern (6, 7) and one of the most valuable fish species on the planet (8). Juveniles exhibit two life-history strategies: residency in the western Pacific, or migration to the eastern Pacific, where they remain for 1 to 4 years (9, 10) before returning to the western Pacific to spawn. Electronic tagging studies have revealed that migrants to the eastern Pacific Ocean make seasonal north-south migrations within the California Current Large Marine Ecosystem (CCLME), along the Mexico and California coasts (10, 11). These movements are consistent with occupation of the routine metabolic thermal minimum zone (10, 12), between 15° and 20°C (minimum rate of oxygen consumption,  $M_{O_2}$ , of 175  $\pm$  29 mg kg<sup>-1</sup> h<sup>-1</sup> at 15°C) (12), and optimization

of aerobic physiological performance, because more energy is required for routine metabolism outside this range. Optimal cardiac performance is also achieved within this thermal window because bradycardia occurs at low temperatures (13), whereas an elevated metabolic rate increases aerobic demands on the heart. To date, the lack of ability to measure foraging success in wild Pacific bluefin tuna has precluded examination of the roles of food availability and physiological mechanisms in driving the migratory cycle (10, 11).

Direct measurement of foraging success in the marine environment is difficult because of the need to simultaneously observe animals at different trophic levels over suitable spatial and temporal scales (14). Electronic tags have been used to infer feeding via a variety of proxies, including movement modes (turning angle and movement speed), whereby sinuous slow movements are interpreted as area-restricted search-type behaviors associated with foraging (15). Other studies have used metrics related to diving behavior as a proxy for feeding, for example, time spent at depth (16), tag immersion in seabirds (17, 18), and descent speed during passive drift dives (which provides a measure of the animal's body condition: larger fat stores confer greater buoyancy) (19). However, in the absence of direct observations, these proxies may not constitute reliable indicators of feeding.

In bluefin tunas, the metabolic heat generated by digestion [the heat increment of feeding (HIF)] is measurable using visceraally implanted archival tags (20) and is strongly correlated with the energetic value of a meal (21, 22). Visceral warming has been used to measure feeding frequency and relative intake size (kg) of feeds in southern bluefin tuna (*Thunnus maccoyii*) in the Indian Ocean (23). Quantitative analyses of feeding in bluefin tunas have hitherto only used estimates of feeding frequency or presence/absence of feeding events (23), which may fail to reveal the true variation in energy intake if the magnitude of feeding events is variable.

Here, we quantify energy intake in 144 wild Pacific bluefin tuna in the CCLME on over 39,000 days (fig. S1), using HIF measurements from implanted archival tags. We estimate energy intake using a model developed with laboratory data collected from similar-sized bluefin tuna (22) at a range of ambient temperatures. This method

<sup>1</sup>Tuna Research and Conservation Center, Stanford University, Hopkins Marine Station, Oceanview Boulevard, Pacific Grove, CA 93950, USA. <sup>2</sup>Sveriges Lantbruksuniversitet, Sötvattenslaboratoriet, Stångholmavägen 2, Drottningholm 178 93, Sweden. <sup>3</sup>Environmental Research Division, Southwest Fisheries Science Center, National Oceanic and Atmospheric Administration (NOAA), 99 Pacific Street, Suite 255A, Monterey, CA 93940, USA. <sup>4</sup>Monterey Bay Aquarium, 886 Cannery Row, Monterey Bay, CA 93940, USA.

\*Corresponding author. E-mail: rebecca.whitlock@slu.se

†Deceased.

accounts for the magnitude of feeding events as well as the effect of ambient temperature on HIF, whereby greater HIF per kcal ingested is observed at cooler ambient temperatures (consistent with greater heat conservation or reduced dissipation at low temperatures). It thus provides a more accurate and robust measure of energy acquisition and foraging success in a wild marine predator than has previously been possible.

## RESULTS

The time series of foraging events in wild Pacific bluefin tuna (median length, 108 cm) as measured by peritoneally implanted archival tags ranged between 61 and 876 days in length (mean, 274 days). The time series data recorded from an archival tagged Pacific bluefin tuna with predicted visceral temperature at rest are shown in Fig. 1 (A to C) (longer time series can be found in figs. S2 and S3). Tracks showing the spatial context for daily energy intake estimates for individual fish are shown in Fig. 2 and fig. S4.

Wild juvenile Pacific bluefin tuna fed successfully on 91% of days (SE, 0.15%). HIF magnitude measured daily varied between 0 and 4106 kcal, with a median of 820 kcal (mean  $\pm$  SD, 855  $\pm$  540 kcal). The daily sea surface temperature (SST) in the CCLME as measured by archival tags varied from 11.0° to 26.7°C (mean  $\pm$  SD, 17.2°  $\pm$  1.8°C) (Fig. 3). Mean thermal excess (the difference between peritoneal and ambient temperature) at the onset of feeding events was 3.7°C ( $\pm$  2.3°C); the maximum 13.8°C. Energy intake and thermal excess were positively correlated with body size as measured by the curved fork length (CFL) of tagged tunas [Pearson correlation coefficients,  $\rho = 0.12$  (HIF),  $\rho = 0.18$  (thermal excess); both significantly different from 0 ( $P < 0.001$ )].

The measurements of energy intake in Pacific bluefin tuna reveal spatial and temporal heterogeneity in foraging success within the

CCLME. Over the course of the year, the highest mean daily energy intake occurred in summer (June and July), when fish are distributed between 23° and 34°N off the coast of the Baja peninsula up to waters of the Southern California Bight (mean  $\pm$  SD, 1034  $\pm$  669 kcal in July) (Figs. 1 and 3 and fig. S1). Lower energy intake was observed during late summer (August and September), when bluefin tuna are moving up through the Southern California Bight (28° to 32°N). A second seasonal peak in energy intake was observed in autumn (October and November), as the Pacific bluefin reach their northernmost distribution at latitudes between 34° and 40°N (Figs. 1 and 3 and fig. S1), coinciding with high primary productivity and cool water temperatures in this region (Fig. 3 and fig. S6). The lowest mean energy intake occurred in December (647  $\pm$  552 kcal), when most Pacific bluefin have returned south of 34°N (Fig. 1 and fig. S1). High energy intake was observed in January and February, when the bluefin's distribution extended northward again (Fig. 1 and fig. S1). In autumn and winter (October to February), the highest energy intake values were observed in the northernmost part of the tuna's range (Fig. 3).

Environmental conditions, spatiotemporal information, and the length of the tagged fish explained a relatively large proportion of the variation in estimated energy intake (adjusted  $R^2$  of 34%) in a generalized additive mixed model (GAMM) (Figs. 4 and 5). Spatial patterns in model-predicted energy intake reflected patterns observed in the raw data (Figs. 1, 3, and 4). Over the year, predicted energy intake was highest in June and July and lowest in December (Fig. 4 and figs. S5 and S6). In autumn and winter (September to March), predicted energy intake increased with latitude, with the highest values predicted north of 32°N in waters off central and southern California (Fig. 4 and fig. S6). In contrast, predicted energy intake was highest at lower latitudes in summer (June and July) (Fig. 4).

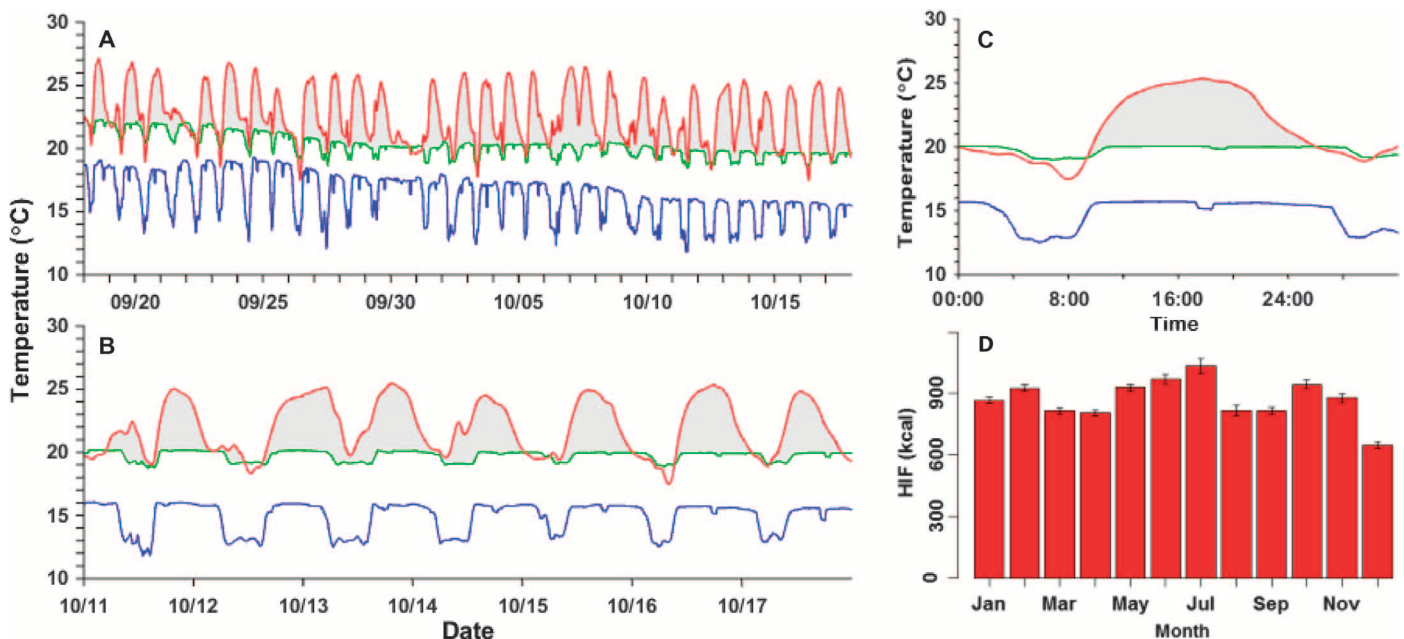


**Fig. 1. Extracts of raw data collected by an archival tag implanted into the peritoneal cavity of a wild juvenile Pacific bluefin tuna in 2003. (A to C)** One month of data (A); 1 week of data (B); one HIF event (over 16 to 17 October) (C). In (A) to (C), the red line shows visceral temperature, the blue line shows ambient temperature, and the green line shows the predicted resting visceral temperature [obtained using a statistical model (22)]. **(D)** Monthly mean HIF from the raw data for archival tagged Pacific bluefin tuna in the California Current between 2002 and 2009. Vertical bars extend to 1.96 SE below and above the mean.



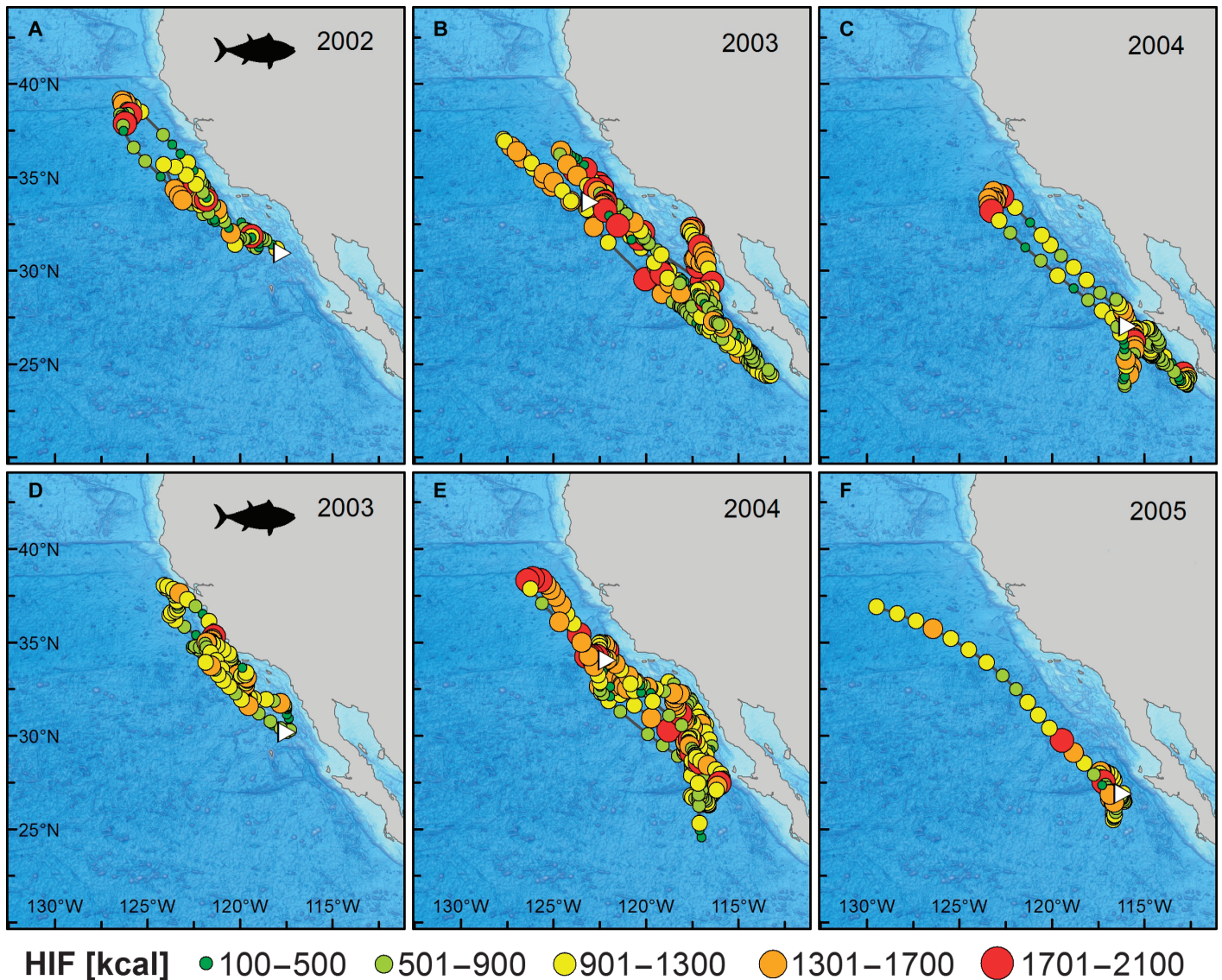


**Fig. 2.** Tracks with estimated HIF ( $\text{kcal day}^{-1}$ ) for two archival tagged bluefin tuna. Tracks are broken into yearly sections, and the first point in each panel is marked with a white triangle. (A to C) HIF track for archival tag 1002020, deployed in August 2002. White triangles correspond to 28 August 2002 (A), 1 January 2003 (B), and 1 January 2004 (C). (D to F) HIF track for archival tag 1003088, deployed in July 2003. White triangles correspond to 7 August 2003 (D), 1 January 2004 (E), and 1 January 2005 (F).

Energy intake was correlated with SST, isothermal layer depth (ILD, an approximation of mixed layer depth), relative light level, chlorophyll-a concentration, length of the tuna, eddy kinetic energy, day of the year, and location (longitude and latitude) (Table 1). Location and SST together explained just over half of the variation in energy intake accounted for by the model (Table 1), whereas season and surface chlorophyll-a concentration each accounted for close to 10% (Table 1). Energy intake was predicted to increase with the length of the tuna (Fig. 5) and decrease with increasing SST and ILD (Fig. 5). Energy intake was predicted to be highest at intermediate levels of primary productivity ( $0.2\text{--}1.0 \text{ mg m}^{-3}$ ), as measured by chlorophyll-a (Fig. 5).

Wild juvenile bluefin tuna maintained a larger difference between peritoneal and ambient temperature (thermal excess) in colder waters

(figs. S2, S3, and S7). Environmental covariates explained 50% of the variation in thermal excess, with most of the variation accounted for by ambient temperature (table S4). Predicted thermal excess showed a similar spatiotemporal pattern to predicted energy intake, generally increasing with latitude except during summer (fig. S7). The fact that SST explained a much higher proportion of the variation in thermal excess than in energy intake (Table 1 and table S4) suggests that our approach was somewhat successful in accounting for the effect of ambient temperature on HIF magnitude and predicted energy intake.

During autumn and winter, the large HIFs observed at high latitudes were accounted for primarily by older, larger fish (Fig. 6 and fig. S8), which were distributed significantly farther north and at significantly colder temperatures in October [age 3 versus age 2 and younger;

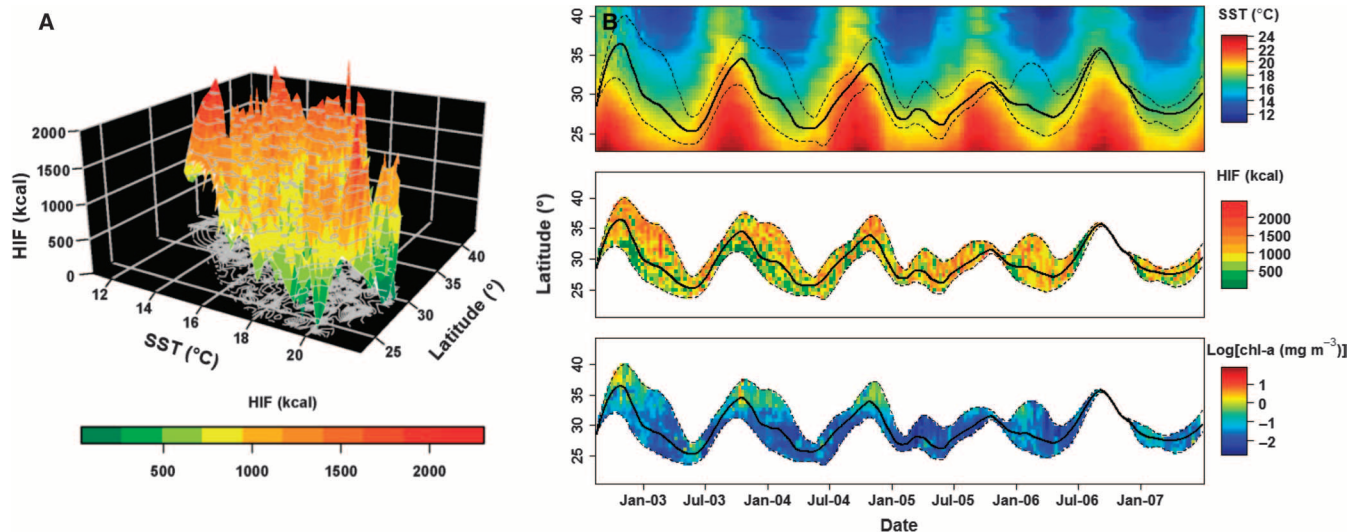


**Fig. 3. HIF in relation to SST, latitude, and chl-a.** (A) Three-dimensional contour plot for observed daily energy intake in 2003 (interpolated and smoothed for visualization) against mean daily SST and latitude. (B) Latitudinal distribution of 144 tagged bluefin tuna in the California Current, 2002 to 2007. (Top) Date versus latitude with remotely sensed mean daily SST ( $^{\circ}\text{C}$ ) indicated by the color scale. (Center) Date versus latitude with median daily energy intake (kcal) indicated by the color scale. (Bottom) Date versus latitude with the logarithm of median daily chlorophyll-a concentration ( $\text{mg m}^{-3}$ ) indicated by the color scale. The solid black line in each panel denotes the median latitude of archival tagged tuna, whereas the dashed lines show the 2.5th and 97.5th percentiles for the latitudinal distribution.

Wilcoxon rank sum ( $W$ ) = 706,168.5 (latitude);  $W$  = 1,138,504 (temperature), both  $P < 0.001$ . The largest size-based differences in energy intake were also observed in October (Fig. 6 and table S3), indicating that thermal niche expansion in this endothermic species results in high energetic reward. Greater utilization of cold waters in a larger fish (11) can be observed in the supplementary raw data traces (figs. S2 and S3).

## DISCUSSION

Optimal foraging theory predicts that animals' movement patterns arise from efficient use of spatially heterogeneous resources and thus reflect the spatial structure of the resource environment. Earlier studies have reported that latitudinal movements of the Pacific bluefin tuna follow seasonal peaks in primary productivity in the CCLME (11) and hypothesized that migrations result from a trade-off between utilizing areas of higher productivity and physiological limitations (of the tuna themselves or their prey) (10). Our direct quantification of energy intake in Pacific bluefin tuna supports the hypothesis that southward movements in winter and spring (coinciding with cooling waters in the north) and northward movements in autumn (coinciding with warming waters in the south) enable the bluefin to remain within a metabolically optimal range, enhancing the availability of excess aerobic capacity for foraging and activity. Average energy intake in the CCLME is highest in July off the coast of the Baja peninsula, coincident with SST approaching the upper end of the thermal habitat utilized by the Pacific bluefin in the eastern Pacific Ocean (Figs. 1 and 4 and fig. S6). We hypothesize that the increased metabolic scope required to digest the large meals (24) observed at this time, combined with temperatures rising above the metabolic thermal minimum zone (Fig. 3 and figs. S6 and S9), leads to oxygen limitation that drives northward migration. By moving north in late summer and early autumn, along the coast of North America, the Pacific bluefin tuna exploit a seasonal thermal window of  $16^{\circ}$  to  $18^{\circ}\text{C}$  in surface waters off central and northern California (Fig. 3).

This is close to the annual maximum SST in this region (Fig. 3), and in the optimal range for the tuna's metabolic and cardiac performance (12, 13, 25). Our results show high energy intake in these northern waters, following summer upwelling events along the northern California coast.

In winter months, as storms mix the water column and SST drops below  $15^{\circ}\text{C}$  off the Californian coast (Fig. 3), the Pacific bluefin tuna move south into Mexican waters along the Baja peninsula, away from the area of highest predicted energy intake in the region of  $34^{\circ}\text{N}$  (Fig. 4). We hypothesize that elevated metabolic costs (fig. S9), coupled with a reduction in cardiac performance at SSTs below  $15^{\circ}\text{C}$  (12, 13, 25) (fig. S9), outweigh potential gains from higher energy intake in northern waters. Size-based differences in thermal habitat utilization (table S3) also point to cold-related physiological constraints: larger fish have greater thermal inertia and increased cardiac capacity. Overall, the Pacific bluefin's migration within the CCLME appears to maximize energy intake within a thermal range of optimal physiological function (fig. S9).

We identified foraging hotspots (areas of seasonally high energy intake) south of  $28^{\circ}\text{N}$  along the Baja peninsula in summer (June and July), off Northern California ( $34^{\circ}$  to  $38^{\circ}\text{N}$ ) in autumn (October and November), and off central California ( $32^{\circ}$  to  $35^{\circ}\text{N}$ ) in winter (January and February) (Fig. 4). Hotspots are likely to have important implications for the management of highly migratory marine species such as *T. orientalis*, for example, as sites of aggregation that are targeted by fishers on account of predictably high densities. Identification of hotspots can also aid in the development of spatially explicit fisheries management strategies or in prioritizing habitats for marine zoning (26, 27). The ability to identify areas of increased feeding success and aggregation is particularly important to inform management for rebuilding depleted populations such as Pacific bluefin tuna. On the basis of our findings, truncation of the population's age/size structure as a result of intense fishing pressure in the CCLME (7) is expected to lead to narrowing of the bluefin's latitudinal distribution (as has already been observed; Fig. 3). A loss of growth potential is also predicted if



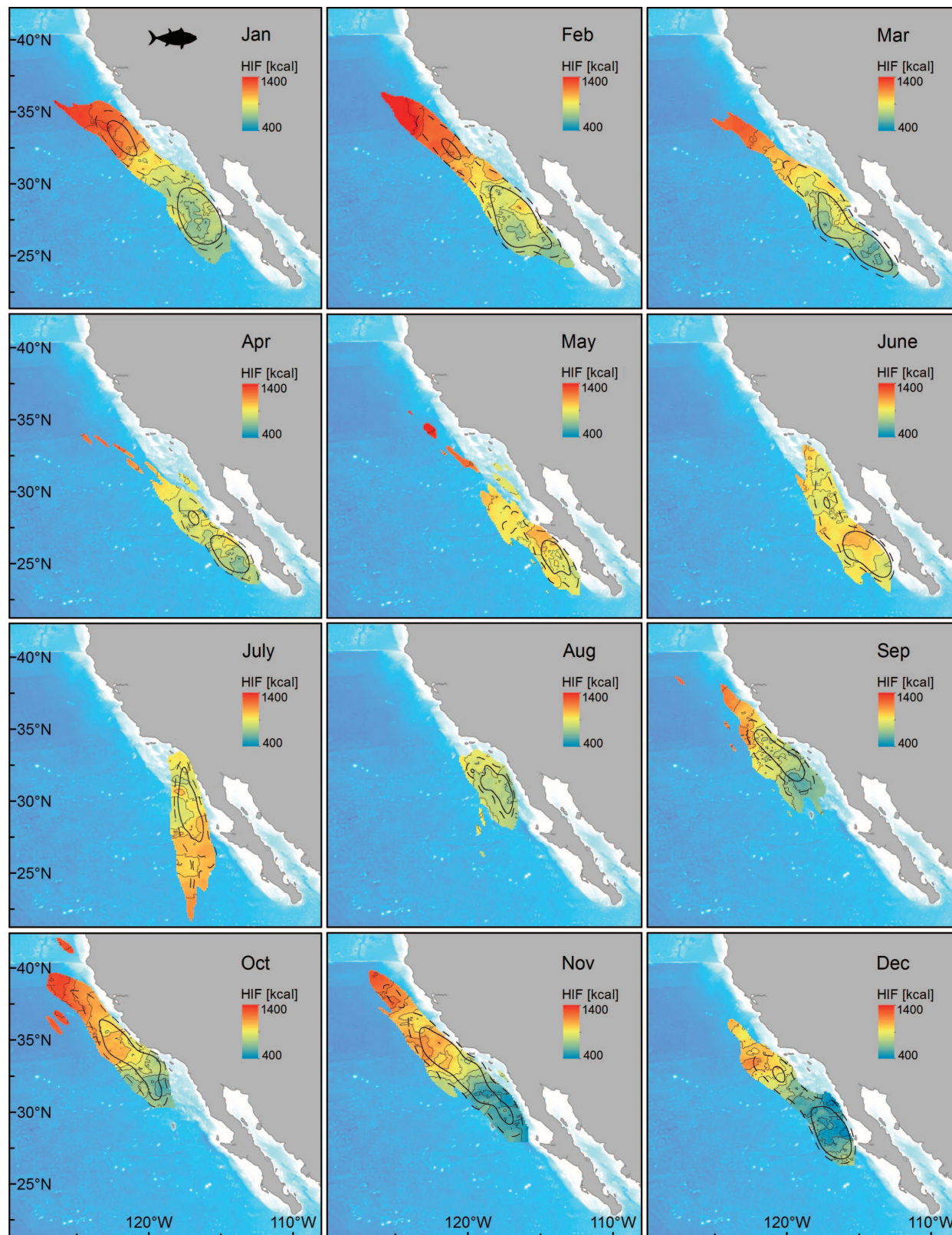


**Fig. 4.** Predicted values for average daily energy intake (kcal) by month from the final GAMM fitted to HIF data between 2002 and 2009 (data from 144 archival tagged Pacific bluefin tuna with 5961 weekly values of HIF). Predicted values are plotted within the 90% utilization density (UD) contour; the 50% (solid line) and 75% (dashed) line UD contours are indicated.

fish do not achieve the body size necessary to access the richest foraging areas in autumn and winter.

Our study also revealed periods of reduced foraging or low foraging success; for example, both individuals in figs. S2 and S3 showed periods with very few HIF events during August (B panels), and late October to November (C panels). In August, this appeared to be associated with northward migration (figs. S2 and S3), perhaps indicating a cessation of feeding during transit between energy-rich foraging grounds, or rapid movement through areas with a high density of predators (10). In October to November, reduced foraging was associated with short southward

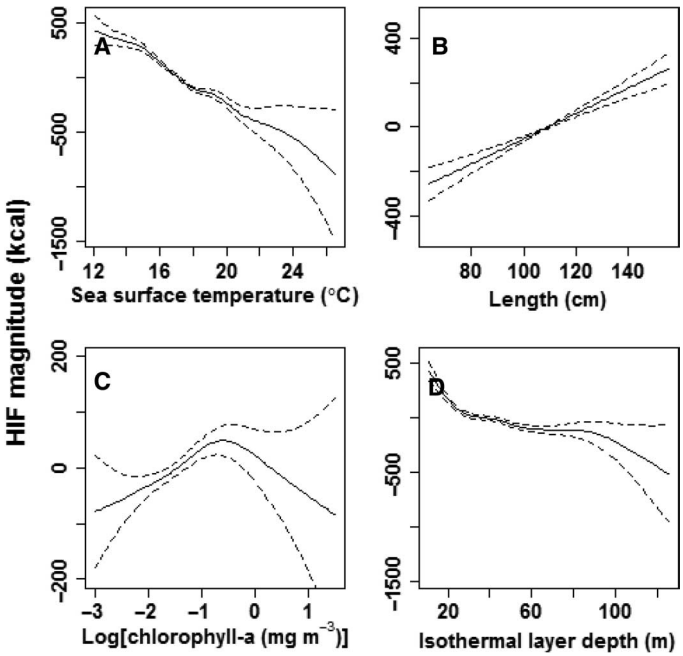


**Fig. 5. Correlates of average daily energy intake (kcal) in tagged Pacific bluefin tuna.** Estimated response curves (smooth terms) and year effects from the final GAMM. (A to D) SST (A), length of the tagged tuna (B), chlorophyll-a concentration (C), and isothermal layer depth (D). Dashed lines represent 95% confidence limits. Vertical axes are partial responses (estimated, centered smooth functions) on the scale of the linear predictor.

movements into warmer waters, which were followed by movement north into colder waters again (figs. S2 and S3). This behavior is consistent with the bluefin tuna seeking a “thermal refuge” in between periods of foraging in cold water.

Our results have important implications for predicting the responses of an apex marine predator to changes in the marine environment, addressing a key knowledge gap (28). By combining the first quantification of energy intake in tuna with knowledge of physiological mechanisms, our approach contributes valuable insight into how the migration phenology and habitat use of Pacific bluefin will respond to changes in ocean temperature. Pacific bluefin tuna appear to face a trade-off between energy intake and physiological performance (fig. S9) that shapes migrations in the CCLME. Several of the tuna’s teleost prey species likely face similar physiological thresholds, so that temperature may serve both as a direct physiological driver and as a proxy for the migratory behavior of prey fishes (29). Changes in water temperature may alter the timing and location of suitable thermal habitats, altering the balance between the costs and benefits of migration [for example, if trophic mismatch (30) results]. A shift in the bioenergetics of migration could result in changes to the population dynamics of Pacific bluefin tuna (via changes in rates of growth and mortality) with cascading effects on lower trophic levels. More research is thus needed into the bioenergetics of migration in this species.

Our direct estimates of energy intake in a highly migratory pelagic predator open up a number of avenues for future research, including the bioenergetics of migration and growth, integration of the preyscape (for example, sardine density) with oceanography and feeding success, and predicting how environmental change will affect the CCLME ecosystem via foraging and migration in an apex predator. Combining predator and prey data using the quantitative metrics of foraging success presented here provides the opportunity for novel testing of the principles of foraging theory in the marine system.

MATERIALS AND METHODS

Archival tags (Lotek, LTD 2310 series A-D) were surgically implanted in juvenile Pacific bluefin tuna captured on hook and line during cruises off the coast of California and Mexico aboard the fishing vessel

**Table 1. Correlates of the magnitude of weekly average energy intake.** Entries are approximate percentage deviance explained by term (of the total deviance explained by the model) for the final GAMM for daily energy intake (kcal), adjusted  $R^2 = 34\%$ .

GAMM term	Approximate deviance explained (%)	Estimated degrees of freedom	Approximate significance level
Year (factor)	3	NA	See fig. S5
s(Latitude, longitude)	27	26.7	$P < 0.001$
s(Sea surface temperature, °C)	26	6.7	$P < 0.001$
s(Isothermal layer depth, m)	3	6.8	$P < 0.001$
s[Log(chlorophyll-a, $\text{mg m}^{-3}$ )]	10	3.3	$P < 0.001$
s(Eddy kinetic energy, $\text{cm}^2 \text{s}^{-2}$ )	4	1.0	$P < 0.001$
s(Relative light level)	9	7.9	$P < 0.001$
s(Length, cm)	8	1.3	$P < 0.001$
s(Day of the year)	12	12.9	$P < 0.001$



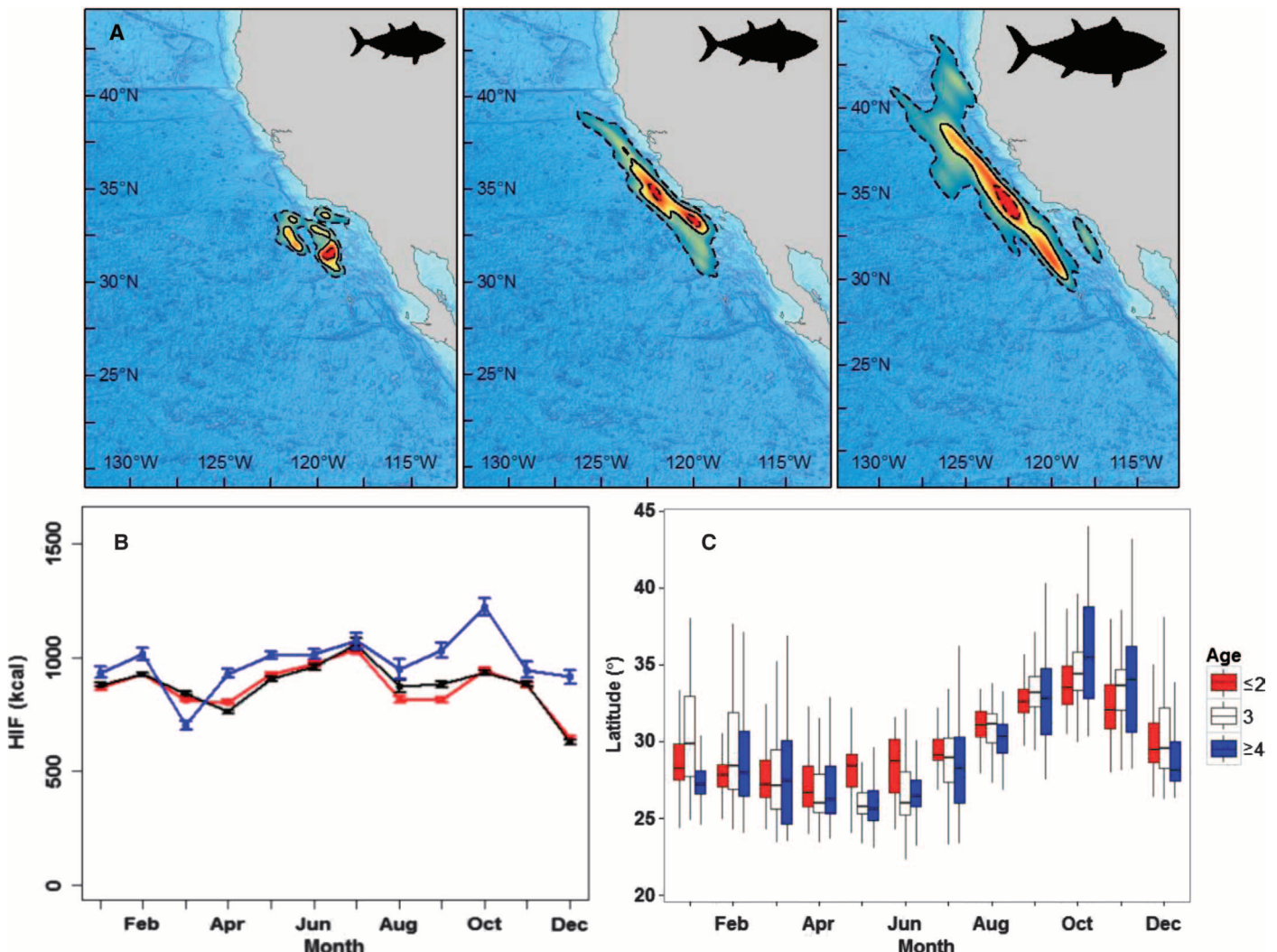


**Fig. 6. Patterns of habitat use and energy intake by length for archival tagged Pacific bluefin tuna between 2002 and 2009.** (A) Utilization densities for archival tagged Pacific bluefin tuna in the California Current in October solid line, 50% density contour; dashed lines, 10 and 90% density contours left 95 cm and smaller; center 95 to 119 cm; right larger than 119 cm. (B) Mean HIF by month and age class (age 2.5 and younger, red; age 2.5-3.5, black; age 3.5 and older, blue). Error bars indicate  $\pm 1$  SE. (C) Boxplots showing the monthly latitudinal distributions of Pacific bluefin tuna of different ages in the California Current (age 2.5 and younger, red; age 2.5-3.5, white; older than 3.5 years, blue). Horizontal lines through the center of each box denote the median, whereas the ends of the box denote the upper and lower quartiles. Whiskers denote the range containing 95% of observations.

Shogun. Implanted archival tags were programmed to record ambient temperature, peritoneal temperature, light, and depth at intervals ranging between 8 and 120 s. Shipboard tagging protocols have been described previously (9–11). CFLs were measured in the tagging cradle for all electronically tagged fish; lengths at release ranged from 59 to 148 cm (mean, 109 cm), corresponding to an age range of about 1 to 5 years (31). The first 6 days of each track were discarded to allow for the fact that feeding patterns may have been altered immediately after tagging due to stress associated with capture, surgery, and release (some individuals were observed not to feed in the first few days after release). Similarly, data from the day on which fish were recaptured were discarded.

Mean daily SST (calculated as the average of ambient temperature readings in the top 3 m of the water column over a 24-hour period), daily HIF magnitude (HIF summed over 24 hours), and mean daily baseline thermal excess [the average predicted baseline peritoneal temperature (22) at the onset of HIF events over a 24-hour period minus the mean

daily SST] were recorded for all tagged Pacific bluefin tuna in the data set. Mean thermal excess was recorded to help interpret patterns in HIF; it is expected to reflect primarily changes in heat production and/or heat conservation at different ambient temperatures (9). We apply a slightly modified version of the hierarchical Bayesian model (HBM) (22) that uses a log-normal observation model to ensure that posterior predictive distributions for HIF do not contain negative values. Results from the two models are comparable [details of the modified model and a comparison with results from the original model (22) can be found in the Supplementary Methods and fig. S10]. The time series of ambient, peritoneal, and predicted baseline peritoneal temperature were plotted for each recovered tag to verify that the algorithm used to predict baseline peritoneal temperature performed satisfactorily. The predicted baseline peritoneal temperature series selected by the algorithm was replaced over short durations in cases where an alternative baseline temperature series offered a better fit to the observed peritoneal temperature values.

Daily energy intake for wild fish was obtained as the posterior predictive distribution for a new individual (that is, an archival-tagged Pacific bluefin tuna for which no experimental observations exist) from the HBM, given measured HIF area and SST (see Supplementary Methods). All estimates of energy intake are reported as the median of the posterior predictive distribution. The results presented in this paper assume a diet of sardines (*Sardinops sagax*) or forage fish of similar nutritional composition (22). A justification for this assumption and a discussion of its implications for our results can be found in the Supplementary Materials.

Daily position estimates were obtained using light-based geolocation methods refined by comparing tag and satellite-observed SST (10, 32). We use location estimates that have been filtered with a Bayesian state-space model (33) to account for observation error and interpolate missing location observations.

Satellite-derived environmental data were extracted on the basis of the 95% posterior probability intervals for daily positions from the state-space model. A suite of remotely sensed environmental variables (SST, sea surface height, sea surface height SD, surface chlorophyll-*a*, eddy kinetic energy, and wind stress curl) were sampled at a daily time scale at each position along the track using Xtractomatic (<http://coastwatch.pfsl.noaa.gov/xtracto/>), and were explored for normalcy and collinearity using QQ plots, variance inflation factors, and scatterplots among variables. Mean ILD (*m*) was also computed for each day (34), using the archival tag profile of ambient temperature and depth and a  $\Delta T$  of 0.8°C.

Weekly means (or geometric means where appropriate) were computed for HIF magnitude, thermal excess, and oceanographic variables. We applied GAMMs (35) to examine the relationships of (weekly mean) daily energy intake or thermal excess with the oceanographic variables described above, time (year and season) and space (latitude and longitude). All models included individual Pacific bluefin tuna as a random effect (random intercept). The results from GAMMs applied directly to the daily data are presented in the Supplementary Materials.

A normal error structure with identity link was used to look at patterns in average daily HIF and thermal excess (after selecting a suitable distribution on the basis of maximum likelihood). Estimated length (based on length at tagging and growth according to a von Bertalanffy model) was included as a covariate in all GAMMs to account for the effect of body size on HIF.

Selection of environmental variables for inclusion in GAMMs was based on the estimated degrees of freedom for smooth terms, estimated significance level, and proportion of the total deviance explained. Thin plate regression splines with shrinkage (35) were estimated for each oceanographic variable. Seasonal effects were modeled by including year day as an explanatory variable in GAMMs using a cyclic cubic regression spline, which constrains the start and end points of the smooth to be the same (35). Correlation of residuals was addressed by including a first-order autoregressive (AR1) error structure for random effects (nested within individual). To account for spatial autocorrelation, an isotropic thin plate regression spline of latitude and longitude was applied, with the maximum dimension of the basis (*k*) used to represent the smooth terms (limiting the maximum degrees of freedom for each model term) set to 50. Akaike's information criterion was used to compare alternative model structures. To approximate the deviance explained by each term in the fixed effects part of GAMMs, generalized additive models were fitted for the full model, null model (intercept only), and submodels in which one smooth term was

dropped at a time. To make a comparison with the full model, smoothing parameters for the remaining terms in the submodels were set equal to their estimates from the full model. Deviance explained for term *i* can then be calculated as the difference between the deviance explained by the full model and submodel lacking *i*, divided by the deviance explained by the null model.

For the purpose of this analysis, the HIF data set was restricted to data from Pacific bluefin tuna with a time at liberty of 50 days or more. We analyze data from the CCLME, defined to include all observations east of the 130th meridian west. We used data from archival tags with complete and uncorrupted body temperature ( $T_B$ ) and ambient temperature ( $T_A$ ) time series and more than 50 days at large ( $N = 183$ ). Data from tags for which baseline thermal excess could not be approximated satisfactorily were discarded, resulting in a HIF data set from 144 wild Pacific bluefin tuna.

To examine size-based differences in the HIF and the distribution of bluefin tuna, individuals were assigned to one of three length classes (31) as follows:  $\leq 94.6$  cm (age 2.5 and younger); age 3,  $> 94.6$  cm and  $\leq 119.2$  cm (age 2.5 to 3.5);  $> 119.2$  cm (older than age 3.5).

## SUPPLEMENTARY MATERIALS

Supplementary material for this article is available at <http://advances.sciencemag.org/cgi/content/full/1/8/e1400270/DC1>

Fig. S1. Spatial plot of the data set analyzed in this paper by month.

Fig. S2. Raw data (visceral temperature, red line; ambient temperature, blue line) trace from an archival tagged Pacific bluefin tuna.

Fig. S3. Raw data (visceral temperature, red line; ambient temperature, blue line) trace from a second archival tagged Pacific bluefin tuna.

Fig. S4. Tracks with estimated median HIF ( $\text{kcal day}^{-1}$ ) for two archival tagged Pacific bluefin tuna.

Fig. S5. Correlates of average daily energy intake (kcal) in tagged Pacific bluefin tuna.

Fig. S6. HIF in relation to SST, latitude, and chl-*a*.

Fig. S7. Predicted values for weekly mean thermal excess ( $^{\circ}\text{C}$ ) plotted by quarter from the final GAMM fitted to thermal excess data between 2002 and 2009 (data from 144 archival tagged Pacific bluefin tuna with 5961 weekly values of thermal excess).

Fig. S8. Patterns of habitat use and energy intake by length for archival tagged Pacific bluefin tuna between 2002 and 2009.

Fig. S9. Physiological responses to ambient temperature with mean energy intake.

Fig. S10. Boxplot of posterior predictive probability distributions for estimated energy intake (kcal) for three archival tagged Pacific bluefin tuna in the feeding experiment (22).

Fig. S11. Histograms of HIF magnitude observations.

Fig. S12. Estimated smooth terms from the GAMM for feeding success in archival tagged Pacific bluefin tuna.

Fig. S13. Predicted feeding success between September 2002 and August 2003 from the binomial GAMM for a subset of archival tagged Pacific bluefin tuna (23 tagged individuals, 6705 observations) released in August 2002.

Fig. S14. Predicted HIF magnitude (conditional on feeding on a given day) between September 2002 and August 2003 from the Gamma GAMM for a subset of archival tagged Pacific bluefin tuna (23 tagged individuals, 6212 observations) released in August 2002.

Fig. S15. GAMM-predicted values from the delta-gamma model for HIF magnitude (combining predictions of feeding success and HIF magnitude) between September 2002 and August 2003 for a subset of archival tagged Pacific bluefin tuna (23 tagged individuals, 6212 observations) released in August 2002.

Table S1. Proximate analysis of sardine and anchovy used as feeds for captive tuna, reproduced from Farwell (43).

Table S2. Priors in the hierarchical Bayesian regression model.

Table S3. Wilcoxon rank sums (from two-sided tests) for size-based differences in latitude, SST, and HIF.

Table S4. Correlates of thermal excess.

References (36–43)

## REFERENCES AND NOTES

1. A. M. Springer, J. A. Estes, G. B. van Vliet, T. M. Williams, D. F. Doak, E. M. Danner, K. A. Forney, B. Pfister, Sequential megafaunal collapse in the North Pacific Ocean: An ongoing legacy of industrial whaling? *Proc. Natl. Acad. Sci. U.S.A.* **100**, 12223–12228 (2003).



2. R. A. Myers, J. K. Baum, T. D. Shepherd, S. P. Powers, C. H. Peterson, Cascading effects of the loss of apex predatory sharks from a coastal ocean. *Science* **315**, 1846–1850 (2007).
3. E. L. Hazen, S. Jorgensen, R. R. Rykaczewski, S. J. Bograd, D. G. Foley, I. D. Jonsen, S. A. Shaffer, J. P. Dunne, D. P. Costa, L. B. Crowder, B. A. Block, Predicted habitat shifts of Pacific top predators in a changing climate. *Nature Clim. Change* **3**, 234–238 (2013).
4. H. O. Pörtner, A. P. Farrell, Physiology and climate change. *Science* **322**, 690–692 (2008).
5. J. R. Brett, Energetic responses of salmon to temperature. A study of some thermal relations in the physiology and freshwater ecology of sockeye salmon (*Oncorhynchus nerka*). *Am. Zool.* **11**, 99–113 (1971).
6. International Scientific Committee for Tuna and Tuna-like Species in the North Pacific Ocean. Stock assessment of Pacific bluefin tuna. Pacific Bluefin Tuna Working Group (2014).
7. R. E. Whitlock, M. K. McAllister, B. A. Block, Estimating fishing and natural mortality rates for Pacific bluefin tuna (*Thunnus thynnus orientalis*) using electronic tagging data. *Fish. Res.* **119–120**, 115–127 (2012).
8. B. B. Collette, K. E. Carpenter, B. A. Polidoro, M. J. Juan-Jordá, A. Boustany, D. J. Die, C. Elfes, W. Fox, J. Graves, L. R. Harrison, R. McManus, C. V. Mente-Vera, R. Nelson, V. Restrepo, J. Schratwieser, C. L. Sun, A. Amorim, P. M. Brick, C. Canales, G. Cardenas, S. K. Chang, W. C. Chiang, L. N. de Oliveira Jr, H. Harwell, R. Lessa, F. L. Fredou, H. A. Oxenford, R. Serra, K. T. Shao, R. Sumaila, S. P. Wang, R. Watson, E. Yáñez, High value and long life—Double jeopardy for tunas and billfishes. *Science* **333**, 291–292 (2011).
9. T. Kitagawa, A. M. Boustany, C. J. Farwell, T. D. Williams, M. R. Castleton, B. A. Block, Horizontal and vertical movements of juvenile bluefin tuna (*Thunnus orientalis*) in relation to seasons and oceanographic conditions in the eastern Pacific Ocean. *Fish. Oceanogr.* **16**, 409–421 (2007).
10. B. A. Block, I. D. Jonsen, S. J. Jorgensen, A. J. Winship, S. A. Shaffer, S. J. Bograd, E. L. Hazen, D. G. Foley, G. A. Brees, A.-L. Harrison, J. E. Ganong, A. Swithenbank, M. Castleton, H. Dewar, B. R. Mate, G. L. Shillinger, K. M. Schaefer, S. R. Benson, M. J. Weise, R. W. Henry, D. P. Costa, Tracking apex marine predator movements in a dynamic ocean. *Nature* **475**, 86–90 (2011).
11. A. M. Boustany, R. Matteson, M. Castleton, C. Farwell, B. A. Block, Movements of Pacific bluefin tuna (*Thunnus orientalis*) in the Eastern North Pacific revealed with archival tags. *Prog. Oceanogr.* **86**, 94–104 (2010).
12. J. M. Blank, J. M. Morrisette, C. Farwell, M. Price, R. J. Schallert, B. A. Block, Temperature effects on metabolic rate of juvenile Pacific bluefin tuna *Thunnus orientalis*. *J. Exp. Biol.* **210**, 4254–4261 (2007).
13. J. M. Blank, J. M. Morrisette, A. M. Landeira-Fernandez, S. B. Blackwell, T. D. Williams, B. A. Block, In situ cardiac performance of Pacific bluefin tuna hearts in response to acute temperature change. *J. Exp. Biol.* **207**, 881–890 (2004).
14. D. A. Croll, B. Marinovic, S. Benson, F. P. Chavez, N. Black, R. Ternullo, B. R. Tershy, From wind to whales: Trophic links in a coastal upwelling system. *Mar. Ecol. Prog. Ser.* **289**, 117–130 (2005).
15. I. D. Jonsen, J. M. Flemming, R. A. Myers, Robust state–space modeling of animal movement data. *Ecology* **86**, 2874–2880 (2005).
16. S. L. Fowler, D. Costa, J. Arnould, N. Gales, C. Kuhn, Ontogeny of diving behaviour in the Australian sea lion: Trials of adolescence in a late bloomer. *J. Anim. Ecol.* **75**, 358–367 (2006).
17. B. Dean, R. Freeman, H. Kirk, K. Leonard, R. A. Phillips, C. M. Perrins, T. Guilford, Behavioural mapping of a pelagic seabird: Combining multiple sensors and a hidden Markov Model reveals the distribution of at-sea behaviour. *J. R. Soc. Interface* **10**, 20120570 (2013).
18. S. L. Watwood, P. J. O. Miller, M. Johnson, P. L. Madsen, P. L. Tyack, Deep-diving foraging behaviour of sperm whales (*Physeter macrocephalus*). *J. Anim. Ecol.* **75**, 814–825 (2006).
19. M. Biuw, B. McConnell, C. Bradshaw, H. Burton, M. Fedak, Blubber and buoyancy: Monitoring the body condition of free-ranging seals using simple dive characteristics. *J. Exp. Biol.* **206**, 3405–3423 (2003).
20. F. G. Carey, J. W. Kanwisher, E. D. Stevens, Bluefin tuna warm their viscera during digestion. *J. Exp. Biol.* **109**, 1–20 (1984).
21. J. Gunn, J. Hartog, K. Rough, The relationship between food intake and visceral warming in southern bluefin tuna (*Thunnus maccoyii*). In *Electronic Tagging and Tracking in Marine Fisheries*, J. R. Sibert and J. L. Nielsen, Eds. (Kluwer Academic Publishers, Dordrecht, 2001), vol. 1, pp.109–130.
22. R. E. Whitlock, A. Walli, P. Cermeño, L. E. Rodriguez, C. Farwell, B. A. Block, Quantifying energy intake in Pacific bluefin tuna (*Thunnus orientalis*) using the heat increment of feeding. *J. Exp. Biol.* **216**, 4109–4123 (2013).
23. S. Bestley, T. A. Patterson, M. A. Hindell, J. S. Gunn, Feeding ecology of wild migratory tunas revealed by archival tag records of visceral warming. *J. Anim. Ecol.* **77**, 1223–1233 (2008).
24. T. D. Clark, W. T. Brandt, J. Nogueira, L. E. Rodriguez, M. Price, C. J. Farwell, B. A. Block, Postprandial metabolism of Pacific bluefin tuna (*Thunnus orientalis*). *J. Exp. Biol.* **213**, 2379–2385 (2010).
25. H. Shiels, G. Galli, B. Block, Cardiac function in an endothermic fish: Cellular mechanisms for overcoming acute thermal challenges during diving. *Proc. Biol. Sci.* **282**, 20141989 (2015).
26. S. K. Hooker, L. R. Gerber, Marine reserves as a tool for ecosystem-based management: The potential importance of megafauna. *Bioscience* **54**, 27–39 (2004).
27. E. L. Hazen, R. M. Suryan, J. A. Santora, S. J. Bograd, Y. Watanuki, R. P. Wilson, Scales and mechanisms of marine hotspot formation. *Mar. Ecol. Prog. Ser.* **487**, 177–183 (2013).
28. A. J. Richardson, C. J. Brown, K. Brander, J. F. Bruno, L. Buckley, M. T. Burrows, C. M. Duarte, B. S. Halpern, O. Hoegh-Guldberg, J. Holding, C. V. Kappel, W. Kiessling, P. J. Moore, M. I. O'Connor, J. M. Pandolfi, C. Parmesan, D. S. Schoeman, F. Schwing, W. J. Sydeman, E. S. Poloczanska, Climate change and marine life. *Biol. Lett.* **8**, 907–909 (2012).
29. D. A. Demer, J. P. Zwolinski, K. A. Byers, G. R. Cutter, J. S. Renfree, T. S. Sessions, B. J. Macewicz, Prediction and confirmation of seasonal migration of Pacific sardine (*Sardinops sagax*) in the California Current Ecosystem. *Fish. Bull.* **110**, 52–70 (2012).
30. M. Edwards, A. J. Richardson, Impact of climate change on marine pelagic phenology and trophic mismatch. *Nature* **430**, 881–884 (2004).
31. T. Shimose, T. Tanabe, K.-S. Chen, C.-C. Hsu, Age determination and growth of Pacific bluefin tuna, *Thunnus orientalis*, off Japan and Taiwan. *Fish. Res.* **100**, 134–139 (2009).
32. S. L. H. Teo, A. Boustany, S. Blackwell, A. Walli, K. C. Weng, B. A. Block, Validation of geo-location estimates based on light level and sea surface temperature from electronic tags. *Mar. Ecol. Prog. Ser.* **283**, 81–98 (2004).
33. A. J. Winship, S. J. Jorgensen, S. A. Shaffer, I. D. Jonsen, P. W. Robinson, D. P. Costa, B. A. Block, State-space framework for estimating measurement error from double-tagging telemetry experiments. *Methods Ecol. Evol.* **3**, 291–302 (2012).
34. A. B. Kara, P. A. Rochford, H. E. Hurlburt, An optimal definition for ocean mixed layer depth. *J. Geophys. Res.* **105**, 16803–16821 (2000).
35. S. Wood, *Generalized Additive Models: An Introduction with R* (CRC Press, Boca Raton, FL, 2006).
36. L. Pinkas, M. S. Oliphant, I. L. K. Iverson, Food Habits of Albacore, Bluefin Tuna, and Bonito in California Waters (Fish Bulletin 152, California Department of Fish and Game, CA, 1971).
37. D. J. Madigan, A. B. Carlisle, H. Dewar, O. E. Snodgrass, S. Y. Litvin, F. Micheli, B. A. Block, Stable isotope analysis challenges wasp-waist food web assumptions in an upwelling pelagic ecosystem. *Sci. Rep.* **2**, 654 (2012).
38. G. Stefánsson, Analysis of groundfish survey abundance data: Combining the GLM and delta approaches. *ICES J. Mar. Sci.* **53**, 577–588 (1996).
39. M. Pennington, Efficient estimators of abundance, for fish and plankton surveys. *Biometrics* **39**, 281–286 (1983).
40. S. C. Barry, A. H. Welsh, Generalized additive modeling and zero-inflated count data. *Ecol. Model.* **157**, 179–188 (2002).
41. S. Wood, F. Scheipl, *gamm4: Generalized additive mixed models using mgcv and lme4. R package version 0.2-2*, 2013; <http://CRAN.R-project.org/package=gamm4>.
42. S. N. Wood, Fast stable restricted maximum likelihood and marginal likelihood estimation of semiparametric generalized linear models. *J. R. Stat. Soc. Ser. B* **73**, 3–36 (2011).
43. B. A. Block, and E. D. Stevens, *Tuna: Physiology, Ecology, and Evolution* (San Diego Academic Press, San Diego, CA, 2001).

**Acknowledgments:** We thank the captains, T. Dunn, N. Kagawa, and B. Smith, and crew of the fishing vessel Shogun for their help with the capture, archival tagging, and release of wild Pacific bluefin tuna. We thank the technical staff of the Tuna Research and Conservation Centre (R. Schallert, J. Nogueira, L. Rodriguez, and students), A. Norton, and the many teams that helped in the tagging efforts through the years. We thank the Mexican government for permitting access to bluefin tunas in Mexican waters for tagging and release and T. Baumgartner McBride, Department of Biological Oceanography, Centro de Investigación Científica y de Educación Superior de Ensenada (CICESE) University, for his support. We are grateful to G. Lawson for making available his code to extract isothermal layer depth and for helpful discussions in the early stages of this work. J. Blank made available data on heart rate and metabolic rate in juvenile Pacific bluefin tuna, for which we are grateful. We would like to thank A. Swithenbank for assistance in automating the HIF measurement code to run through the Pacific bluefin tuna archival tag data set. R. Whitlock provided helpful comments on an earlier version of the manuscript. We thank the two anonymous reviewers for their insightful and constructive comments that helped us to improve the manuscript. **Funding:** This research was supported by the Moore, Packard, and Monterey Bay Aquarium Foundations, and by a NOAA Fisheries and the Environment (FATE) grant. **Author contributions:** R.E.W.: Co-conceived the project, quantified energy intake and tag-based statistics, analyzed the data, GAMMs, drafted the manuscript, edited the manuscript, plotting. E.L.H.: GAMMs, interpreted oceanographic data, contributed text, edited the manuscript, plotting. A.W.: Contributed to the analytical framework and to MATLAB code to quantify energy intake. C.F.: tagging of bluefin tuna, oversight of laboratory work, edited the manuscript. S.J.B.: oceanographic expertise, edited the manuscript. D.G.F.: Extracted and analyzed the oceanographic data, oceanographic expertise. M.C.: Plotting, edited the manuscript. B.A.B.: Co-conceived the project, archival tagging of bluefin tuna, contributed to the analytical framework and writing of the manuscript, edited the manuscript. **Competing interests:** The authors declare that they have no competing interests. **Data and materials availability:** Codes for quantification of HIF from archival tag ambient and peritoneal temperature data and GAMM analyses can be obtained on request from the first author.

Submitted 29 December 2014

Accepted 1 July 2015

Published 25 September 2015

10.1126/sciadv.1400270

**Citation:** R. E. Whitlock, E. L. Hazen, A. Walli, C. Farwell, S. J. Bograd, D. G. Foley, M. Castleton, B. A. Block, Direct quantification of energy intake in an apex marine predator suggests physiology is a key driver of migrations. *Sci. Adv.* **1**, e1400270 (2015).

This article is published under a Creative Commons license. The specific license under which this article is published is noted on the first page.

For articles published under [CC BY](#) licenses, you may freely distribute, adapt, or reuse the article, including for commercial purposes, provided you give proper attribution.

For articles published under [CC BY-NC](#) licenses, you may distribute, adapt, or reuse the article for non-commercial purposes. Commercial use requires prior permission from the American Association for the Advancement of Science (AAAS). You may request permission by clicking [here](#).

**The following resources related to this article are available online at <http://advances.sciencemag.org>. (This information is current as of September 25, 2015):**

**Updated information and services**, including high-resolution figures, can be found in the online version of this article at:  
<http://advances.sciencemag.org/content/1/8/e1400270.full.html>

**Supporting Online Material** can be found at:  
<http://advances.sciencemag.org/content/suppl/2015/09/22/1.8.e1400270.DC1.html>

This article **cites 37 articles**, 15 of which you can be accessed free:  
<http://advances.sciencemag.org/content/1/8/e1400270#BIBL>

*Science Advances* (ISSN 2375-2548) publishes new articles weekly. The journal is published by the American Association for the Advancement of Science (AAAS), 1200 New York Avenue NW, Washington, DC 20005. Copyright is held by the Authors unless stated otherwise. AAAS is the exclusive licensee. The title *Science Advances* is a registered trademark of AAAS